TUTA/IOE/PCU

Journal of the Institute of Engineering, 2019, ***15(1):*** *38-47*
© TUTA/IOE/PCU
Printed in Nepal

Electrical and Thermal Characterisation of Millscale Modified Sn-Cu Lead-Free Solders

Olatunde Sekunowo, Stephen Durowaye, Gbenga Fashakin
Department of Metallurgical and Materials Engineering, University of Lagos, Nigeria
Corresponding author: *sdurowaye@unilag.edu.ng*

Received: *Sep 24, 2018* **Revised:** *Nov 25, 2018* **Accepted:** *Dec 2, 2018*

Abstract: Lead-free solders are gaining much attention as a result of legislation against the inclusion of lead and other hazardous materials in solders used in joining electronic components. This study investigated the effect of iron millscale (IMS) modified tin-copper (Sn-Cu) alloy on the electrical resistivity, electrical, and thermal conductivities of the solder samples under increasing applied current. The input materials consist of tin, zinc and iron millscale while the copper was varied from 0.2 – 1.0 wt. %. Fabrication of the alloy employed metal casting technique followed by relevant test samples preparation for characterisation in terms of microstructure, electrical, and thermal conductivities. Results show that the sample with 1 wt. % Cu addition exhibited the highest electrical and thermal conductivity values of 9967.9 S/m and 11.24 x 10^{-5} W/mK respectively at applied current value of 600 A with the lowest resistivity of 1 x 10^{-4} (Ωm). The solder alloy microstructure confirmed the presence of Cu_6Sn_5-FeO intermetallic phase dispersed in Sn matrix forming a continuous network. Contribution to the overall desirable performance of the solder alloy may have stemmed from the strong and coherent inter-crystal cohesion between the Cu_6Sn_3 and FeO phases which resulted in improved electrical and thermal conductivities of the as cast solder. The grade of solder alloy fabricated is adjudged suitable for assembling electronic components in industrial plant control panels.

Keywords: Lead-free solder, iron millscale, microstructure, electrical property, thermal property

1. Introduction

Traditionally, a solder is an alloy containing about 40% lead (Pb) and 60% tin (Sn). The fume produced by the flux of such solder is usually toxic causing a wide range of harmful effects especially as it concerns issues having to do with human health [3, 4]. Although in application, a typical lead based solder forms fume that is clearly visible as white smoke but readily degenerates to irritant gasses on further thermal treatment. Hence, the restriction on the use of lead based solder in the electronics industry. This has led to extensive research and development efforts aimed at improving reliability and properties of Sn based solders. Furthermore, given that Sn is non-toxic, its combination with other allied elements is desirable and capable of guaranteed good solderability. Currently, there are many lead-free solder alloy formulations that have been developed for use in the

electrical and electronic industries [11]. Based on the industry practice, these alloy formulations are being made to converge on the ternary eutectic of Sn-Ag-Cu (SAC) alloy exhibiting approximately 227^0 C eutectic temperature for reflow and Sn 0.7 Cu alloy having eutectic temperature of 227^0 C for wave soldering. It is generally believed that the different variations of the Sn-Ag-Cu (SAC) alloy with silver content from 3 – 4 % are all acceptable compositions.

SAC solders have also been reported to outperformed high lead (Pb) solders joints in several structures including ceramic ball-grid array (CBGA) system [5, 8]. For example, the ball-grid arrays with a ceramic substrate showed consistently better result in thermal cycling for Pb-free alloys. It also appears to be more resistant to gold embrittlement than Sn-Pb. Furthermore, the strength of the joints was substantially higher for the SAC alloys than Sn-Pb alloys. Thus, SAC solder alloys have been favoured to replace Sn-Pb solders. However, the currently used ternary eutectic of 217^0 C or near eutectic SAC solders has some drawbacks. According to Kang et al. [10], most SAC solders often exhibit a relatively high amount of undercooling (10–30^0C), as β-Sn requires large undercooling to nucleate and solidify. This large undercooling promotes the formation of large, plate-like Ag_3Sn structures that have been reported to cause joint embrittlement and reliability problem [12].

Research has been done on solders with lower silver content. For example, Sn-1.0 Ag-0.5 Cu (SAC 105) in an attempt to inhibit the formation of Ag_3Sn and also to reduce the solder cost as the price of Ag has increased dramatically in recent years [7, 14]. Although, it has been reported that SAC 105 performs better in drop tests, it has a higher liquidus temperature which requires a higher reflow profile than the eutectic Sn-3.8 Ag-0.7 Cu (SAC 387) alloy and also performs poorly in thermal cycling tests [13]. These drawbacks have prompted researchers to modify the solder content by adding small amounts of other alloying elements to further improve its reliability and lower its melting temperature. As part of the global drive to develop lead-free solders, the main objective of this research is to investigate the effect of varied copper (Cu) particles addition on the electrical resistivity, electrical, and thermal conductivities of iron millscale-tin-copper (FeO-Sn-Cu) solder for application in the electrical and electronics industries.

2. Materials and Methods

2.1 Materials and Apparatus

The materials and apparatus used are iron millscale (IMS), tin, and copper while crucible pots, pit furnace, cylindrical metallic moulds, optical microscope, micro-ohm meter, ammeter, and arc spectrometer, infrared thermometer are the equipment used. Pictures of some of these materials are presented in Fig. 1 and Fig. 2.

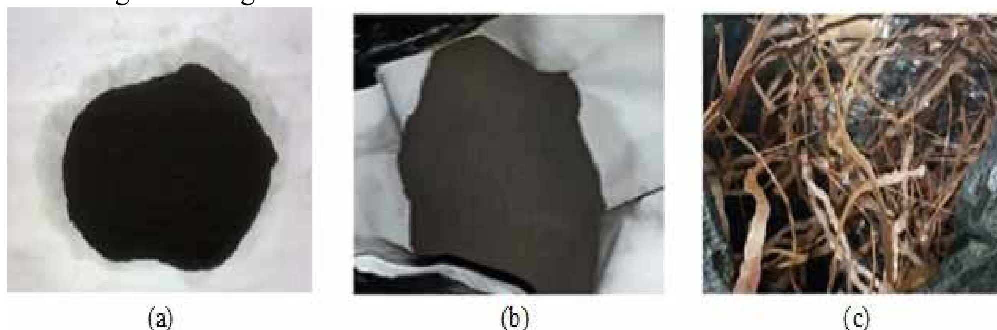

Fig. 1: Pictures of materials used (a) iron millscale (b) tin (c) copper wire

2.2 Melting and Casting

Measured quantities of the input materials were mechanically blended and divided into five portions and identified as samples 1 – 5 as illustrated in Tables 1a and 1b. The samples were preheated to 150^0 C in five crucible pots (Fig. 2a) to remove moisture and prevent explosion. The crucible pots containing the input materials were then charged into a pit furnace (Fig. 2b) and heated until molten. This was followed by thorough stirring for 2 mins using a long stainless steel rod to avoid clustering and to achieve homogeneity. The melt was then cast in cylindrical metallic moulds of diameter 0.8 cm and length 10 cm (Fig. 2c), allowed to cool in the moulds after which the cast samples were stripped from the moulds.

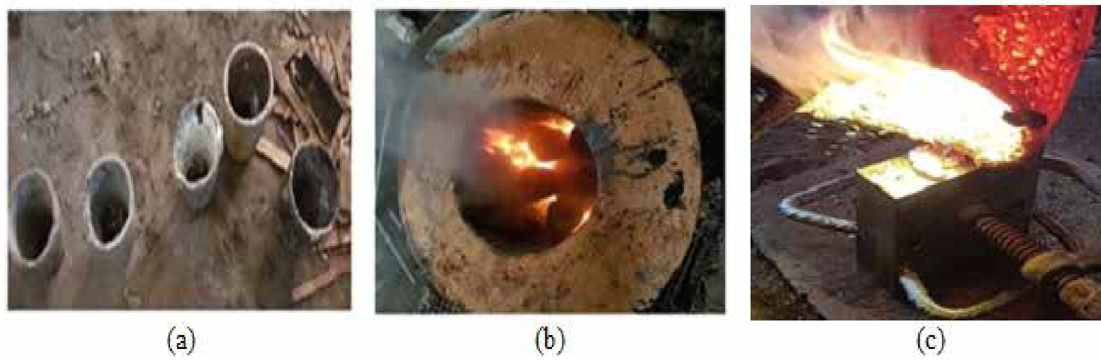

Fig. 2: (a) Preheated crucible pots, (b) Pit furnace, (c) Cylindrical metallic moulds containing the melt

Table 1a: Materials formulation

Samples/Materials	Tin (Sn) (wt. %)	Millscale (FeO) (wt. %)	Copper (Cu) (wt. %)	Total (wt. %)
Sample 1	98.8	1	0.2	100
Sample 2	97.6	2	0.4	100
Sample 3	96.4	3	0.6	100
Sample 4	95.2	4	0.8	100
Sample 5	94.0	5	1.0	100

Table 1b: Materials formulation

Samples/Materials	Tin (Sn) (g)	Millscale (FeO) (g)	Copper (Cu) (g)	Total (g)
Sample 1	109.07	1.11	0.27	110.45
Sample 2	107.75	2.21	0.54	110.50
Sample 3	106.65	3.31	0.81	110.77
Sample 4	105.03	4.42	1.08	110.53
Sample 5	103.77	5.52	1.35	110.64

Table 2: Composition analysis of the as cast solder in wt. %

Element	Sample 1	Sample 2	Sample 3	Sample 4	Sample 5
Al	0.0698	0.0711	0.0689	0.0697	0.0701
Si	0.3032	0.3051	0.2958	0.3082	0.2989
Ti	0.1308	0.1314	0.1321	0.1318	0.1324
P	0.0891	0.0872	0.0885	0.0896	0.0874
Mn	0.0118	0.0114	0.0117	0.0119	0.0114
Fe	0.1067	0.1206	0.1387	0.1437	0.1507
Ni	0.0987	0.0965	0.0957	0.0968	0.0972
Cu	1.1225	1.3347	1.4758	1.4864	1.5585
Zn	0.5153	0.5148	0.5142	0.5121	0.5119
Nb	0.0061	0.0059	0.0056	0.0058	0.0063
Sn	97.035	96.811	96.662	96.632	96.565
Sb	0.5109	0.5103	0.5112	0.5117	0.5105

2.3 Characterisation of the Solder Samples

The elemental composition (Table 3) of the as cast samples was determined using a bench top arc spectrometer Model 120971/06 while the microstructural examination of samples was carried out using an optical microscope, Model CETI 0703552. The experimental set-up of Fig. 3 illustrates the procedure adopted in determining the electrical resistivity of the test samples. The test was carried out at ambient temperature using a DV powered micro-ohm meter RM0600 machine varying current from 10 – 610 A. The electrical resistivity ($\rho\rho$) and conductivity (C) of the samples were obtained applying Equations 1 and 2 [6].

$$\rho = R\frac{A}{L} \qquad (1)$$

ρ = resistivity (Ω)' R = resistance (Ω)

A = cross − sectional area of the sample (cm^2)listance between 2 leads of voltmeter(V)

$$C = \frac{1}{\rho} \qquad (2)$$

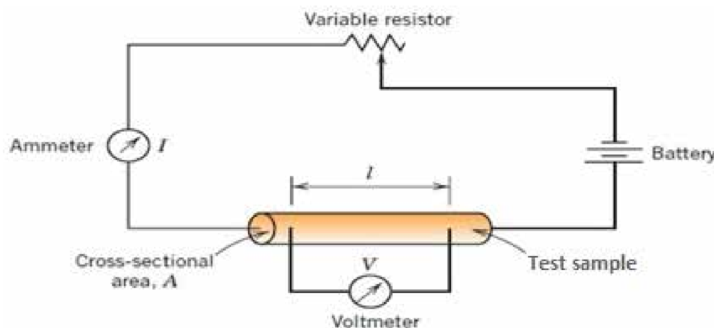

Fig. 3: Experimental set-up for the electrical resistivity testing

Thermal conductivity of the solder samples was determined in accordance with ASTM C177 standard. Each of the samples was heated using an electric hot plate of power input 750 W for 20 mins after which the test sample was removed and the temperature $(T_A)(T_A)$ of the side in direct contact with the hot plate and temperature $(T_B)(T_B)$ of the top surface of the sample were quickly measured using an infrared thermometer. The thermal conductivity was calculated using Equations 3 and 4 [9].

$$K = \frac{Qx \quad Qx}{At\Delta TAt\Delta T} \tag{3}$$

$$Q = p - Q_{loss}Q = p - Q_{loss} \tag{4}$$

where K = Thermal conductivity of the sample in W/mK, Q = Quantity of heat flowing through the sample in J, $Q_{loss} = Q_{loss}$ = Parasitic heat loss to the surrounding by conduction and radiation which is approximately 2 % of the heat flow through the sample, p = Power input in W, x = Thickness of the sample in m, A = Cross-sectional area of the sample in m^2, t = Time in seconds, $\Delta T \Delta T$ = Temperature difference$(T_A - T_B)$ in K$(T_A - T_B)$ in K, $T_A T_A$ = Temperature of the side of the sample that is in direct contact with the hot steel plate in K, $T_B T_B$ = Temperature of the top surface of the sample in K.

2.4 Hardness Evaluation

The cast solder alloy bars were thoroughly fettled preparatory to hardness properties test. Three different points on the samples surfaces where subjected to hardness test using the Vickers scale.

3. Results and Discussion

3.1 Microstructure

The elemental composition of the as cast samples presented in Table 2 shows that Sn is the dominant element followed by Cu and Fe respectively. The phase diagram of the Sn–Cu system in Fig. 4 shows a eutectic reaction at the composition Sn–0.7 wt.% Cu and at temperature of 227^0 C. The arrow points the eutectic composition Sn–0.7 wt. % Cu and eutectic temperature 227^0 C. The eutectic Sn–0.7Cu alloy is one of the Sn-based lead free solder alloys having small amounts of Cu–Sn intermetallic compound precipitated in the Sn matrix. The eutectic reaction occurred between the intermetallic compound Cu_6Sn_5 and Sn. The microstructure as predicted from the phase diagram consists of β-Sn and the Cu–Sn intermetallic compound Cu_6Sn_5 [2].

It is observed that all the micrographs of the as-cast iron millscale-tin-copper (FeO-Sn-Cu) solder in Figs. 5a, 5b, and 5c reveal highly dense regions containing FeO and both Cu and Sn. The grey region containing both Sn and Cu represents an intermetallic compound adjudged to be Cu_6Sn_5. The complete molten state of Sn provided a rapid diffusion medium for Cu resulting in the formation of the intermetallic compound. The micrographs show that Sn is present in all the samples whereas Cu, which is only in amount of 0.2 – 1 wt. %, is present where the intermetallic compound, Cu_6Sn_5 is present. With the addition of 0.8 wt. % Cu particles, Cu_6Sn_5 phase is seen distributed in the lighter contrast Sn matrix phase. Figs. 5a, 5b and 5c show the two phase regions of Sn and intermetallic Cu_6Sn_5 with FeO. The regions containing dispersed Cu_6Sn_5-FeO are separated by dendritic regions of Sn matrix, giving the microstructure a network-like appearance. Further increase in the concentration of millscale to 4 wt. % gave rise to an inducement of darker Cu_6Sn_5-FeO phase coupled with a relatively coarse precipitates in Fig. 5b than Fig. 5a. Similar trend is observed as the concentration of Cu and millscale was increased to 1 and 5 wt. % respectively

resulted in increased presence of the dark Cu_6Sn_5-FeO phase in the micrograph (Fig. 5c). It appears the increase in the addition of Cu from 0.2 – 1.0 wt. % enhanced reaction within the Cu–Sn system with a remarkable effect on the electrical and thermal conductivities of the alloy.

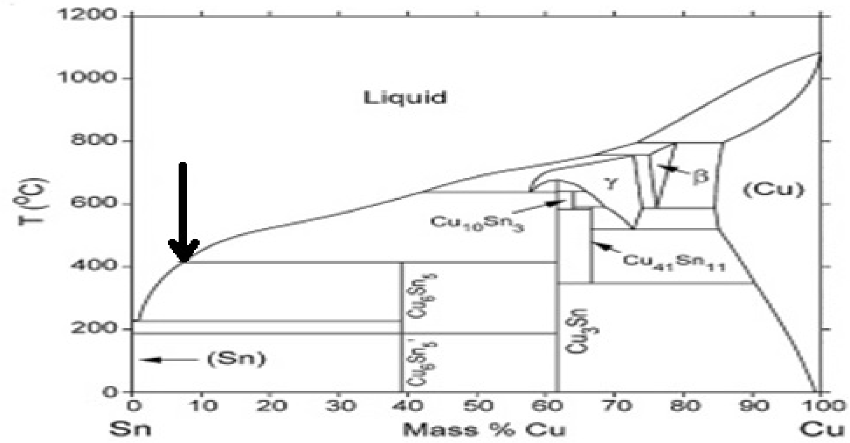

Fig. 4: The Sn–Cu phase diagram [2]

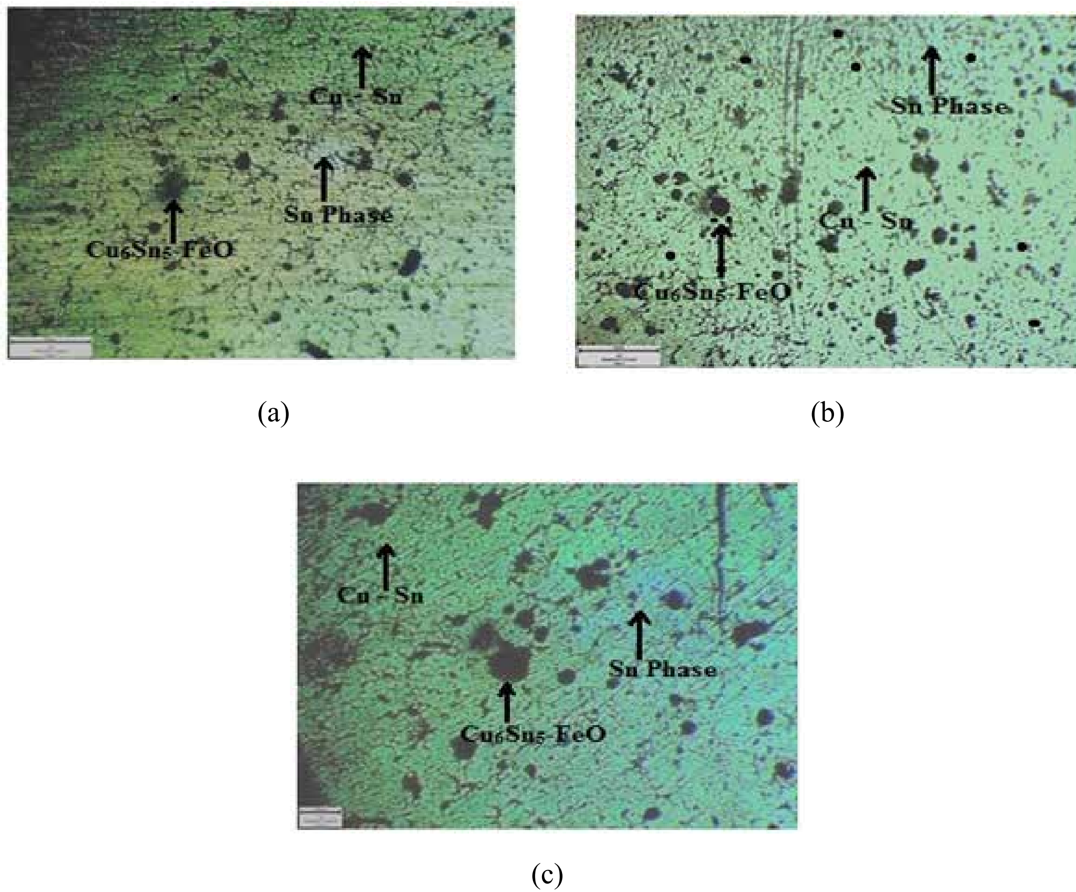

Fig. 5: Optical micrographs of (a) 0.2 wt. % Cu, (b) 0.8 wt. % Cu and (c) 1.0 wt. % Cu. Magnification: 300x

3.2 Electrical and Thermal Conductivities of the Solder Alloy Samples

The electrical and thermal conductivities of the solder alloy are illustrated in Figs. 6 and 7. It is observed that the alloy composition with 1 wt. % Cu exhibited the highest electrical and thermal conductivity values of 9967.9 S/m and 11.24 x 10^{-5} W/mK respectively. The interfacial bonding between the two dominant phases in the alloy's microstructure (Fig. 5c) must have been responsible for the observed performance. Furthermore, there is a steady increase in the electrical conductivity of the samples as applied current (A) increases from 10 to 600 A while the resistivity strength decreases. The higher the electrical conductivity within a material, the greater is the current density for a given applied potential difference [1]. This behaviour may be attributed to the disturbances in the lattice order due to thermal vibration which may cause scattering of conducting electrons. Highly conductive materials such as copper (Cu) silver, (Ag), and aluminium (Al) allow the free movement of electrons within their molecular lattice. Thus, the value of the electrical conductivity depends on the ability of electrons or other charge carriers to move within the lattice. Hence, the addition of copper (Cu) has enhanced the electrical and thermal conductivities of the solder alloy samples.

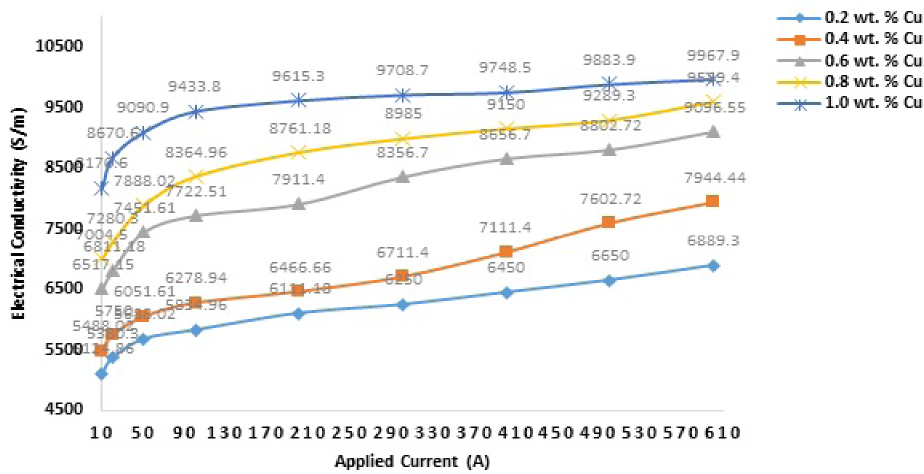

Fig. 6: Effect of varied copper addition on the electrical conductivity of the solder alloy samples with increasing applied current

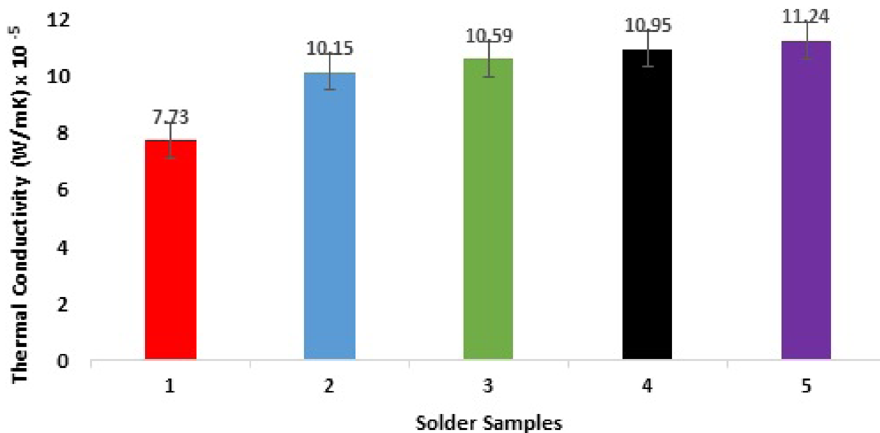

Fig. 7: Effect of varied copper addition on the thermal conductivity of the solder samples

3.3 Electrical Resistivity of the Solder Alloy Samples

As shown in Fig. 8, a steady decrease in the electrical resistivity of the solder alloy samples obtains as applied current (A) increases from 10 to 600 A. This behaviour further validates established relationship between electrical resistivity and electrical conductivity; the former being the inverse of the latter. Sample 5 which contains the highest amount of copper (1 wt. % Cu), exhibited the lowest electrical resistivity value of 1 x 10^{-4} (Ωm) at 600 A while sample 1 containing the lowest amount of copper (0.2 wt. % Cu), exhibited the highest electrical resistivity value of 1.45 x 10^{-4} (Ωm) at 600 A.

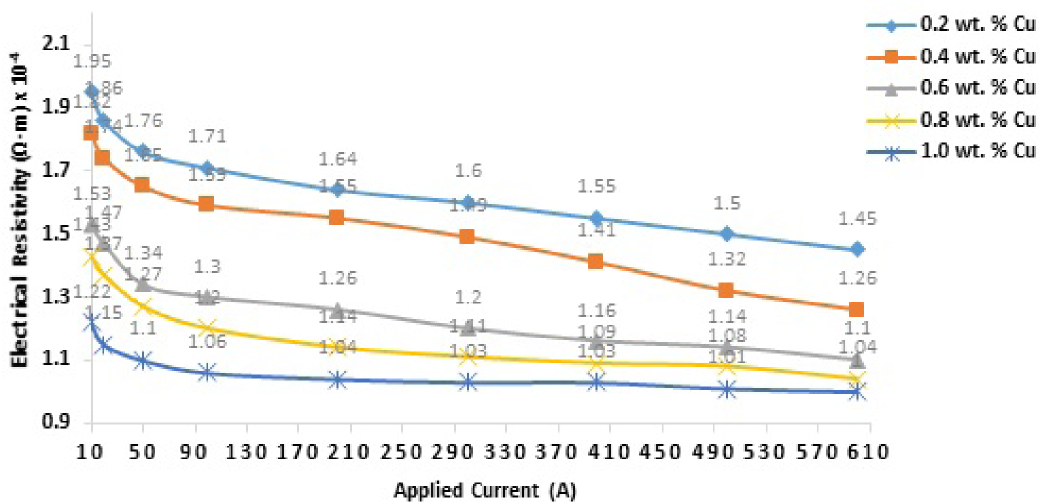

Fig. 8: Effect of varied copper addition on the electrical resistivity of the solder alloy samples with increasing applied current

3.4 Hardness of the As-Cast Solder Alloy

Fig. 9 shows the hardness behaviour of the cast solders. The hardness values were observed to increase as IMS addition increases while the highest hardness of 21.7 HV is demonstrated at 5 wt. % IMS addition. The IMS particles appear to be coherent with the tin matrix and being a harder phase, it effectively enhanced inter-crystal cohesion, which resulted in the observed increase in hardness. This behaviour was found to subsist as the volume fraction of IMS particles increase within the matrix. It is observed from Fig. 9 that the hardness values range from 11.3 – 21.7 HV. This level of hardness appears to be sufficient to prevent any form of damage to soldered joints after solidification. Moreover, the hardness value range obtained in this study compared well with the report of Yee and Haseeb [15] for solders meant for joining electronic components in control panels operating in a relatively high thermal environment.

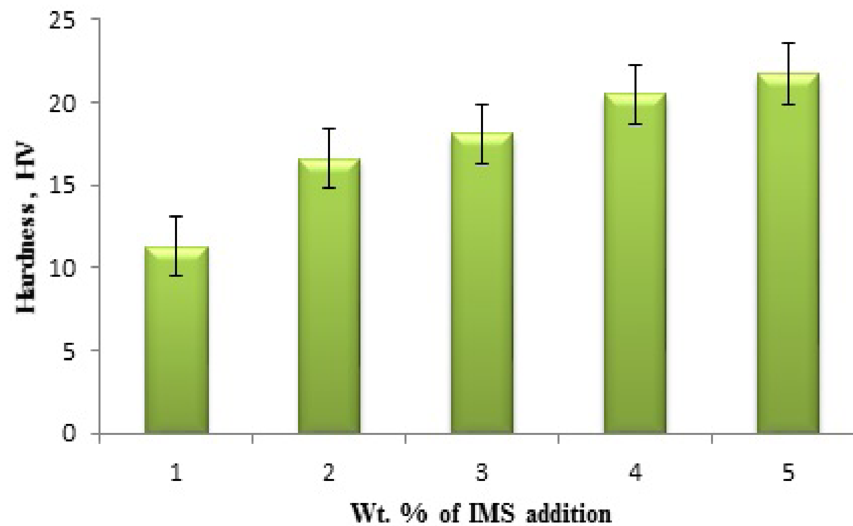

Fig. 9: Effect of IMS particles addition on hardness of Sn-Cu solder alloy

4. Conclusion

The investigation of the electrical and thermal conductivity of iron-millscale modified Sn-Cu solder alloy has been carried out. From the results and their analyses, the following conclusions are drawn:

- The thermal and electrical properties (conductivity and resistivity) of the as-cast solder alloys are generally influenced by the combined and varied concentrations of iron-millscale and copper.
- Increase in copper addition from 0.2 – 1.0 wt. % facilitated effective Cu–Sn reaction coupled with the structure modifying effect of iron-millscale resulted in strong and coherent inter-crystal cohesion. This development conferred improved electrical and thermal conductivity on the solder alloy.
- Given that the solder alloy melts at the range of 240^0 – 250^0 C coupled with the above level of performances, it is adjudged suitable as a joining solder material of electronic components in industrial control panel circuit boards.

References

[1] Ahmad D, Mazil A, Jamaid A and Othman A (2017), Electric field and current density performance analysis of gases as an insulation, *IOP Publishing Limited, IOP Conference Series: Materials Science and Engineering*, **226**: 1-12.

[2] Alam S, Prerna M and Kumar R (2015), Effect of Ag on Sn–Cu and Sn–Zn lead free solders. *Materials Science-Poland*, **33**: 317-330.

[3] Anna K, Ogunseitan O, Saphore J and Schoenunp J (2003), Lead free solders: issues of toxicity, availability and impacts of extraction, *53rd Proceedings of Electronic Components and Technology*, New York, USA, 1-8.

[4] Arab MR, Heidaki MH, Mashnadi MD, Mirzaei R and Jahantigh MD (2011), Histological study of the toxic effects of solder fumes on spermatogenesis in rats. *Cell Journal*, **13**: 5-10.

[5] Brewin A, Hunt C, Dusek M and Nottay J (2002), Reliability of joints formed with mixed alloy solders. *National Physical Laboratory Report MATC (A) 85*, Middlesex, UK, 1-18.

[6] Callister WD and Balasubramaniam R (2011), Materials science and engineering, *7th Edition, Wiley India Pvt. Ltd.*, New Delhi-110002, India, ISBN 978-81-265-2143-2,

[7] Cheng F, Gao F, Zhang J, Jin W and Xiao X (2011), Tensile properties and wettability of SAC0307 and SAC105 low Ag lead free solder alloys. *Journal of Materials Science*, **46**: 3424–3429.

[8] Dhafer AS, Mohd FM and Irfan AB (2012), The limited reliability of board level SAC solder joints under both mechanical and thermo-mechanical loads, *J. of Micro-electronics and Materials*, **42**: 3-10.

[9] Eastop TD and McConkey A (2005), Applied thermodynamics for engineering technologists, *5th Edition, Pearson Education Ltd,* Harlow, United Kingdom, 582–584.

[10] Kang SK, Shih DY, Leonard D, Donald NY, Henderson DW and Gosselin T (2004), Ag_3Sn-plate formation in the solidification of near-ternary eutectic Sn-Ag-Cu, *Journal of the Minerals, Metals & Materials Society (JOM)*, **56**: 34–38.

[11] Lee NC and Bixenman (2015), Lead free: how flux technology will differ, *65th Proceedings of Electronic Components and Technology Conference*, Texas, USA, 1-9.

[12] Leong YM and Haseeb AS (2016), Soldering characteristics and mechanical properties of Sn-1.0 Ag-0.5 Cu solder with minor aluminum addition. *Materials,* **9**: 522.

[13] Liu W and Lee NC (2007), Effects of additives to Sn-Ag-Cu alloys on microstructure and drop impact reliability of solder joints. *Journal of the Minerals, Metals & Materials Society*, **56**: 26–31.

[14] Shnawah DA, Sabri MF, Badruddin LA, Said SB and Che FX (2012), The bulk alloy microstructure and mechanical properties of Sn-1 Ag-0.5 Cu-x Al solders (x = 0, 0.1 and 0.2 wt. %), *Journal* of *Materials Science*: *Materials* in *Electronics,* **23**: 1988–1997.

[15] Yee ML and Haseeb AS (2016), Soldering characteristics and mechanical properties of Sn-1.0Ag-0.5Cu solder with minor aluminium addition, *Journal of Materials*, **9**: 1-17.